Chapter 4 Absorption and reaction of CO_2 in capillaries

Capítulo 4 Absorción y reacción de CO_2 en capilares

PEÑA, Rosaura†[1], HURTADO, Lourdes[2], ROMERO, Rubi[1] and NATIVIDAD, Reyna*[1]

[1]*Chemical Engineering Lab / Centro Conjunto de Investigación en Química Sustentable UAEM-UNAM, Universidad Autónoma del Estado de México*
[2]*Unidad Académica Profesional Acolman, Universidad Autónoma del Estado de México*

ID 1st Author: *Rosaura, Peña* / **ORC ID**: 0000-0001-9184-8477, **CVU CONACYT ID**: 239954

ID 1st Co-author: *Lourdes, Hurtado* / **ORC ID**: 0000-0001-9892-9528, **CVU CONACYT ID**: 368065

ID 2nd Co-author: *Rubi, Romero* / **ORC ID**: 0000-0001-9163-7936, **CVU CONACYT ID**: 121454

ID 3rd Co-author: *Reyna, Natividad* / **ORC ID**: 0000-0001-8978-1066, **CVU CONACYT ID**: 87755

DOI: 10.35429/H.2021.6.51.74

R. Peña, L. Hurtado, R. Romero, and R. Natividad

*rnatividadr@uaemex.mx

A. Marroquín, J. Olivares, M. Ramírez and L. Cruz (Coord) Engineering and Technology. Handbooks-©ECORFAN-México, Querétaro, 2021.

Abstract

The process of carbon dioxide (CO_2) reduction to value-added chemicals is being extensively studied worldwide. The main purpose is to decrease emissions to the environment that are associated with global warming, as well as the creation of renewable and sustainable energy sources. In the aforementioned process, the absorption of CO_2 is of paramount importance as well as the reactor where the CO_2 conversion takes place. In this context, the objective of this chapter is to present and analyze the results of the CO_2 absorption in alkaline solutions in capillary reactors. A hydrodynamic study is included in order to establish the operational window of liquid and gas velocities in order to achieve the Taylor flow regime. All experiments were conducted in a capillary reactor (d_c = 3 mm). The studied variables were temperature, NaOH concentration (0-0.75 M) and capillary length (300 and 100 mm). It was found that the volumetric mass transfer coefficient of the absorption of CO_2 in water increases when the temperature decreases, while the CO_2 absorption in NaOH solutions increases directly with temperature. By means of the Ha number, it was concluded that the mass transfer controlled the absorption process when using alkaline solutions.

CO_2 absorption, capillary reactor, mass transfer, pH, reactive absorption

Resumen

El proceso de reducción de dióxido de carbono (CO_2) a productos químicos de valor agregado se está estudiando ampliamente a nivel mundial. La finalidad principal es disminuir emisiones al medio ambiente, las cuales se asocian al calentamiento global, así como la creación de fuentes de energías renovables y sustentables. En el proceso antes mencionado, la absorción de CO_2 es de suma importancia, así como el reactor donde se realiza la conversión del CO_2. En este contexto, el objetivo de este capítulo es presentar los resultados de la absorción de CO_2 en soluciones alcalinas llevada a cabo en un reactor capilar. Se incluye un estudio hidrodinámico para establecer la ventana de operación de velocidades de líquido y gas para obtener el régimen tipo Taylor. Todos los experimentos se realizaron en un reactor capilar (d_c = 3 mm). Las variables estudiadas fueron temperatura, concentración de NaOH (0-0.75M) y la longitud del capilar (300 y 100 mm). Se encontró que el valor del coeficiente de transferencia de masa si la absorción de CO_2 se realiza en agua incrementa cuando la temperatura disminuye mientras que la absorción en soluciones de NaOH incrementa directamente con la temperatura. Mediante el número de Hatta (Ha) se concluye que la transferencia de masa controla el proceso de absorción cuando se emplean soluciones alcalinas.

Absorción de CO_2, reactor capilar, transferencia de masa, pH, absorción reactiva

1. Introduction

Currently, the conservation of terrestrial ecosystems has attracted the attention of the scientific community due to the fact that damage to these ecosystems because of global warming has been observed. In this context, various research groups have focused on proposing strategies aimed at reducing pollutants in the environment. Global warming is caused by the greenhouse effect, a natural mechanism in which the Earth's atmosphere heats up, and it occurs thanks to the presence of certain gases, including carbon dioxide and other gases present in the air -such as water vapor (H_2O), methane (CH_4), nitrogen oxides (NO, N_2O, NO_2) and ozone (O_3), which are known as greenhouse gases. These gases can absorb solar radiation favoring the increase in temperature in the atmosphere. One of the most important is carbon dioxide since its concentration in the atmosphere is constantly increasing. The exponential increase in anthropogenic activities such as agriculture, industry, indiscriminate felling of trees, destruction of vegetation, the burning of fossil fuels along with the intensive destruction of ecosystems, have caused carbon dioxide emissions to the atmosphere to be greater than the amount required to carry out photosynthesis or the amount of gas that dissolves in ocean waters.

In addition to this, the development of alternative energy sources to replace fossil fuels has focused mainly on the development of clean energy sources, without carbon emissions, such as turbines powered by water and wind and solar energy; however, the drawback with renewable energy sources is the intermittent nature of the energy produced (Mebrahtu et al., 2019).

While the development of alternative sources of energy is in process and in progress, there is also an urgent need to find a solution to mitigate, store or convert the CO_2 produced or emitted to the environment, in order to contribute to CO_2 atmospheric level remains constant or even decreases. Even though this greenhouse gas has several applications, the amount used is minimal. Some of the compounds produced from CO_2 are: urea (for nitrogen fertilizers and plastics), salicylic acid (a pharmaceutical ingredient), polycarbonates (for plastics), ethylene, propylene, carbonates (Centi & Perathoner, 2009). It is also used as a refrigerant, carbonating agent, supercritical solvent, inert medium, pressurizing and neutralizing agent (Ganesh, 2016).

In general, two strategic routes have been proposed to avoid an increase in the concentration of CO_2 in the atmosphere: 1) mitigation and 2) capture and use of CO_2. Regarding the first route, it seeks to minimize CO_2 emissions that come from large facilities such as the cement, metal, bioethanol, oil and petrochemical refining industries, from power plants for the production of electricity, from medium sources such as industrial and commercial buildings and from small sources such as transportation; through different approaches, including the establishment of environmental regulations and the limitation of vehicular traffic. However, these actions are insufficient, because they require improvements in energy efficiency and a shift from fossil fuels to less carbon-intensive energy sources.

The second strategy, capture and use (CCU) to generate value-added chemicals, is particularly interesting as it can alleviate dependence on fossil fuels for energy, while promoting new technical sinks in the cycle biogeochemistry of carbon. In recent years, the use of CO_2 to produce value-added fuels and chemicals has become very important and challenging, mainly because the molecule is chemically stable due to its carbon-oxygen bonds (with a bond enthalpy of C=O +805 kJ/mol) and therefore its conversion to carbon-based fuels requires a large amount of energy to break the bond.

The transformation of CO_2 to chemicals of commercial interest (short chain) such as carbon monoxide (CO), methanol (CH_3OH), formaldehyde (HCHO) and acetic acid (CH_3COOH) and even formic acid (HCOOH) and the formation of fuels such as ethanol (CH_3CH_2OH), methane (CH_4) or hydrogen (H_2), can be carried out by different processes, including biological reduction, electrochemical reduction, photo-catalytic reduction, thermo-catalysis, among others (Ola & Maroto-Valer, 2015). Recent research results also indicate that CO_2 can be used to produce methanol, using it instead of carbon monoxide in the synthesis gas mixture (mixture of carbon monoxide and hydrogen $CO + H_2$) *(Yang et al*., 2017).

The generation of fuels from CO_2 through the photo-reduction process seems to be the most economical and ecological approach for sustainable development because an economic reducing agent such as water can be used, solar energy is available in abundance, there is no generation of toxic products or waste, and little or no carbon emission (Shehzad, Tahir, Johari, & Murugesan, 2018). In this sense, Lourdes Hurtado, Natividad, & García, 2016 demonstrated that the use of capillary reactors, instead of the typical stirred tank reactors, lead to a different distribution of products when the photo-reduction of CO_2 is carried out. Therefore, it is important to study the absorption of this gas in this type of reactors.

Capillary reactors are tubes with internal diameters of 1 to 4 mm. They are distinguished from microreactors because the internal diameter of these latter is less than 1 mm. The option of using a capillary reactor in multiphase reaction processes is supported by the statement that the mass transfer between the phases is intensified, mainly due to the reduction of the contact length between the phases and because it also has the advantage of being able to immobilize the catalyst onto the reactor wall (Natividad *et al*., 2004).

In the capillary reactor ($d_c < 4$ mm), the flow regime is dictated by the flow rates and the properties of the liquid and gas, as well as the diameter of the capillary. The existence of four main flow regimes in a vertical capillary is well known and they are: bubble type, Taylor type (plug), aerated and annular flow (Figure 4.1).

Figure 4.1 Main flow regimes in a capillary a) bubble, b) aerated c) annular, d) Taylor (plug)

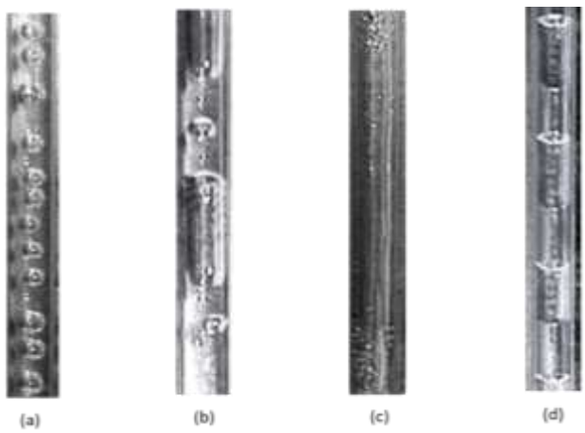

Source: Natividad, PhD thesis, 2004

The Taylor (or plug) flow consists of gas bubbles with a length greater than the diameter of the capillary that move along the tube separated between them by the elongated parts of the liquid. Due to their size, the bubbles leave only a thin film of liquid between the bubble and the wall. One characteristic that makes Taylor flow unique is the micro-mixing pattern found in the liquid segments, this pattern enhances mixing within the liquid phase and eliminates any possible radial concentration gradients. This determines the high efficiency of mass transfer in a capillary reactor (Heiszwolf, Kreutzer, Eijnden, Kapteijn, & Moulijn, 2001; Natividad *et al*., 2004).

In this context, this chapter aims to present the results of the hydrodynamic study of a capillary reactor (d_c = 3 mm) in order to establish the operating window in which the Taylor flow is obtained. Under this operating regime, results of carbon dioxide absorption (CO_2) in aqueous solutions of sodium hydroxide (NaOH) (reactive absorption) are presented. The mass transfer coefficients and the species involved in the reactive absorption process were also calculated.

It is important to mention that reactive absorption has two main advantages: 1) the absorbed solute reduces the partial pressure at equilibrium, improving the driving force between the gas and the interface, 2) the mass transfer coefficient in the liquid phase increases. The theoretical framework for the absorption of CO_2 in aqueous solutions is presented below.

1.1 CO_2 absorption in aqueous solutions

The absorption of CO_2 in water (pH less than 8) is considered purely physical absorption, because when equilibrium is reached, only a small fraction (0.2% - 1%) of the dissolved CO_2 (see Equation 1) is found as carbonic acid: $H_2CO_{3(ac)}$ (Ganesh, 2016), a product of the reaction between molecules (Equation 2). In other words, the equilibrium position prefers carbon dioxide and water ($k_{-1} \gg k_1$) (Holum, 1990; Palmer & Van Eldik, 1983) as it is shown in Figure 4.2, and therefore the CO_2 in the solution remains as molecularly solvated or freely hydrated (Cotton, 1999).

Figure 4.2 $CO_{2\,(ac)} + H_2CO_{3\,(ac)}$ balance

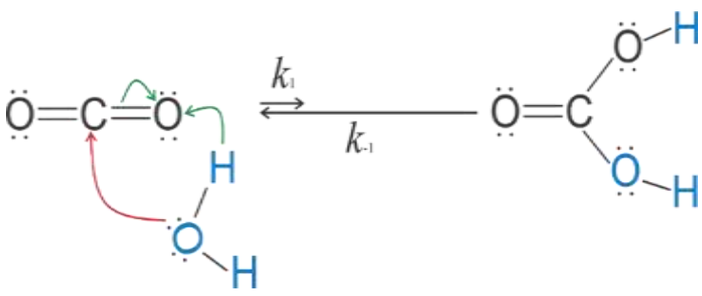

Source: Salgado, Bachelor thesis, 2020

Equilibrium is reached when carbonic acid, which is a weak acid, dissociates twice due to its two protons attached to its oxygen atoms. In the first dissociation (Equation 3) a proton (H^+) and a bicarbonate ion (HCO_3^-) are released, in the second dissociation (Equation 4) the carbonate ion (CO_3^{2-}) is generated and the second H^+ proton is released. If the conjugated bases are not found with another species with a positive charge different from the protons, carbonic acid is formed again. Therefore, it can be asserted that, if the absorption medium is only water, the only species found in solution is dissolved CO_2, for practical purposes $H_2CO_3^*$, without omitting the small amount of carbonic acid formed (Equation 5) (Ganesh, 2016).

$$CO_{2(g)} \leftrightarrow CO_{2(aq)} \quad (1)$$

$$CO_{2\,(aq)} + H_2O \leftrightarrow H_2CO_3^* \quad (2)$$

$$H_2CO_3 \leftrightarrow H^+ + HCO_3^- \quad (3)$$

$$HCO_3^- \leftrightarrow H^+ + CO_3^{2-} \quad (4)$$

$$H_2CO_3^* = H_2CO_{3\,(aq)} + CO_{2\,(aq)} \quad (5)$$

During the reactive absorption of CO_2, the dissolution is carried out in solutions at a pH higher than 8, which is reached when alkaline solutions are used. The presence of cations (Na^+, K^+, Mg^{2+}, Ca^{2+}) and anions (OH^-) in aqueous solution causes that the equilibrium in the reaction $H_2CO_3^*$ is not reached until the reactions between the dissolved ions and the resulting ions of the dissociation reactions of $H_2CO_3^*$ take place (Savage, Astarita, & Joshi, 1980; Shim, Lee, Lee, & Kwak, 2016; Skoog, 2014).

$$H_2CO_3 + OH^- \leftrightarrow HCO_3^- + H_2O \quad (6)$$

$$HCO_3^- + OH^- \leftrightarrow CO_3^{2-} + H_2O \quad (7)$$

The absorption of CO_2 in alkaline aqueous solutions involves fairly rapid homogeneous reactions (Skoog, 2014). The global reactions are presented in Equations 8 and 9,

$$CO_{2(aq)} + 2OH^- \rightarrow CO_3^{2-} + H_2O \quad (8)$$

$$CO_{2\,(aq)} + H_2O + CO_3^{2-} \rightarrow 2HCO_3^- \quad (9)$$

2. Methodology

2.1 Set up of the CO_2 absorption and reaction system

The system used to absorb CO_2 in the capillary reactor was set up according to that described in the patent application MX/Aa/2017/003883 and is described below (see Figure 4.3). At the top of the capillary reactor, a "T" shaped connection was installed to simultaneously feed the liquid and gas phases. In one of the “T” outlets, the quartz capillary with an internal diameter of 3 mm and a length of 300 mm was placed and this was submerged in a 100 mL 3 neck ball flask, the temperature was monitored inside the flask and it was controlled with a thermal bath.

The gas phase was supplied through a stainless-steel pipe and the gas flow was controlled by an AALBORG mass flow controller (model GFC17). A Masterflex peristaltic pump (model 7557-12) with a Masterflex flow controller (model 07557-14) was used to recirculate the liquid phase.

Figure 4.3 Experimental set-up for the absorption of CO_2 (Original image)

Source: "Obtained by the author"

2.2 Hydrodynamic study

The experiment set-up depicted in Figure 4.3 was used to carry out a hydrodynamic study, which consisted in obtaining the velocity operating window for both phases, in order to develop a Taylor flow regime. The experiments were carried out using two different reducing agents: water and a 0.5 M solution of sodium hydroxide. The surface velocity of CO_2 was varied between 0.01 m/s and 0.53 m/s, while the interval of variation of the surface velocity for the liquid phase was set between 0.01 m/s and 0.26 m/s.

Next steps were followed to carry out this study: after the installation of the system, a previous washing was carried out using 60 mL of deionized water and recirculating it through the pipes, connections and the capillary reactor through the peristaltic pump. The temperature was kept constant at each assessed value by using a thermal bath, 60 mL of either water or NaOH solution were added and the flow rate was regulated by adjusting the liquid flow rate in the pump. The reactor CO_2 supply valve was opened, and the speed was adjusted using the mass flow meter. The gas and liquid flow rates were independently changed, and the hydrodynamic regime observed in the capillary reactor was recorded.

2.2.1 Effect of temperature on the hydrodynamics of the system

The experiments were performed at 10 and 25 °C, to determine the effect of this variable on the hydrodynamics of the system, as the section 2.2 indicates, by modifying the temperature under study.

2.3 CO_2 absorption

The effect of three operational variables (temperature, NaOH concentration and reactor length) on CO_2 absorption has been elucidated. This study was carried out with a superficial gas velocity of 0.05 m/s and liquid of 0.08 m/s, these velocities showed a Taylor-type regime, in a capillary with an internal diameter of 3 mm. To determine the effect of temperature on the amount of absorbed CO_2, experiments were carried out at 10, 15, 25, 35 and 40 °C, the concentration of the NaOH solution was 0.5 M. The effect of NaOH concentration on the CO_2 absorption was established by performing experiments with solutions of different initial concentration (0.25, 0.5 and 0.75 M), in this case the temperature was kept constant at 25 °C.

For the study of both variables, temperature and NaOH concentration, a 300 mm length quartz capillary was used. An additional experiment was carried out at a temperature of 25 °C and a solution with a molar concentration of NaOH of 0.5M, using a 100 mm capillary in order to establish the effect of the length of the capillary reactor. In all cases, the response variable was the amount of CO_2 absorbed in the solutions, which, in turn, was used to estimate the mass transfer coefficients between the different phases.

CO_2 quantification was carried out by means of a volumetric analysis with a standardized acid solution. This technique is known as the Warder method (Grzelka, Sobieszuk, Pohorecki, & Cygan, 2011). This method is very useful to differentiate and quantify the species that participate in the reactive absorption process and in this way to study the behavior of the species involved in the capillary reactor (CO_2, H_2CO_3, CO_3^{2-} and HCO_3^-). Methyl orange and phenolphthalein were used as indicators (with pH ranges of 3.1-4.4 and 8.3 -10, respectively), the titration was carried out with a 0.1M sulfuric acid solution standardized with Na_2CO_3 solutions.

3. Results

3.1 Hydrodinamic study in the capillary reactor

The study of the hydrodynamics of the system was limited to establish the surface velocity of the fluids to obtain the operating window in which each of the possible flow regimes illustrated in Figure 4.1 (annular, bubble, aerated or Taylor flow) is obtained. The Taylor or plug type flow is presented in Figure 4.4.

Figure 4.4 Taylor flow in a capillary reactor (d_C= 3mm) (Original image)

Source: "Obtained by the author"

The flow of the gas phase and the liquid phase was gradually varied, keeping one of the two flows constant. Its conversion to surface velocity allowed establishing a map of hydrodynamic regimes for a capillary with an internal diameter of 3 mm and a length of 300 mm, handling a liquid temperature of 10 and 25 °C. In the study, several two-phase flow patterns were observed; the resulting flow patterns are shown in Graphic 4.1.

In general, for all conditions, at a relatively low gas velocity (u_G) a Taylor flow was noticed, which is described by an alternating arrangement of liquid plugs and elongated bubbles with a length greater than the diameter of the capillary and separated from the wall of the capillary tube by a very thin film of liquid. The occurrence of periodic instabilities led to a phenomenon that periodically broke the elongated bubble and created an unstable slug zone (Graphic 4.1a and 4.1b).

This effect occurs with an increase in u_G, which led to a greater amplitude of the velocity of recirculation of gas bubbles, but on the contrary, increasing liquid velocity (u_L) led to a rapid flow of liquid creating a fast plug zone (Graphic 4.1a and 4.1b). The annular flow was the only regime observed in all the conditions studied (Graphic 4.1a, 4.1b, 4.1c and 4.1c) at a relatively higher u_G, for this type of flow the liquid phase does not collide with the gas phase and instead has a continuous flow. A gas core surrounded by a liquid film or even with periodic interfacial waves were observed (annular-wavy). These interfacial waves become less dominant at higher gas concentrations but less liquid flow, becoming an aerated type (Graphic 4.1c).

Moreover, in Graphic 1, we can observe that operating at low temperature (10 °C) and low gas velocity (0.01 m/s), there is a larger operating window to obtain the plug type flow than operating at 25 °C. This behavior is observed when using both water and 0.5M NaOH. This hydrodynamic regime is the one of greatest interest in this work, for which an operating window for both phases was determined and Table 4.1 summarizes the operating conditions to operate in a Taylor-type regime.

Graphic 4.1 Flow regimes map in the 300 mm length and 3 mm internal diameter quartz capillary, using a) water at 10 °C, b) water at 25 °C, c) NaOH 0.5M at 10 °C and d) 0.5M NaOH at 25 °C

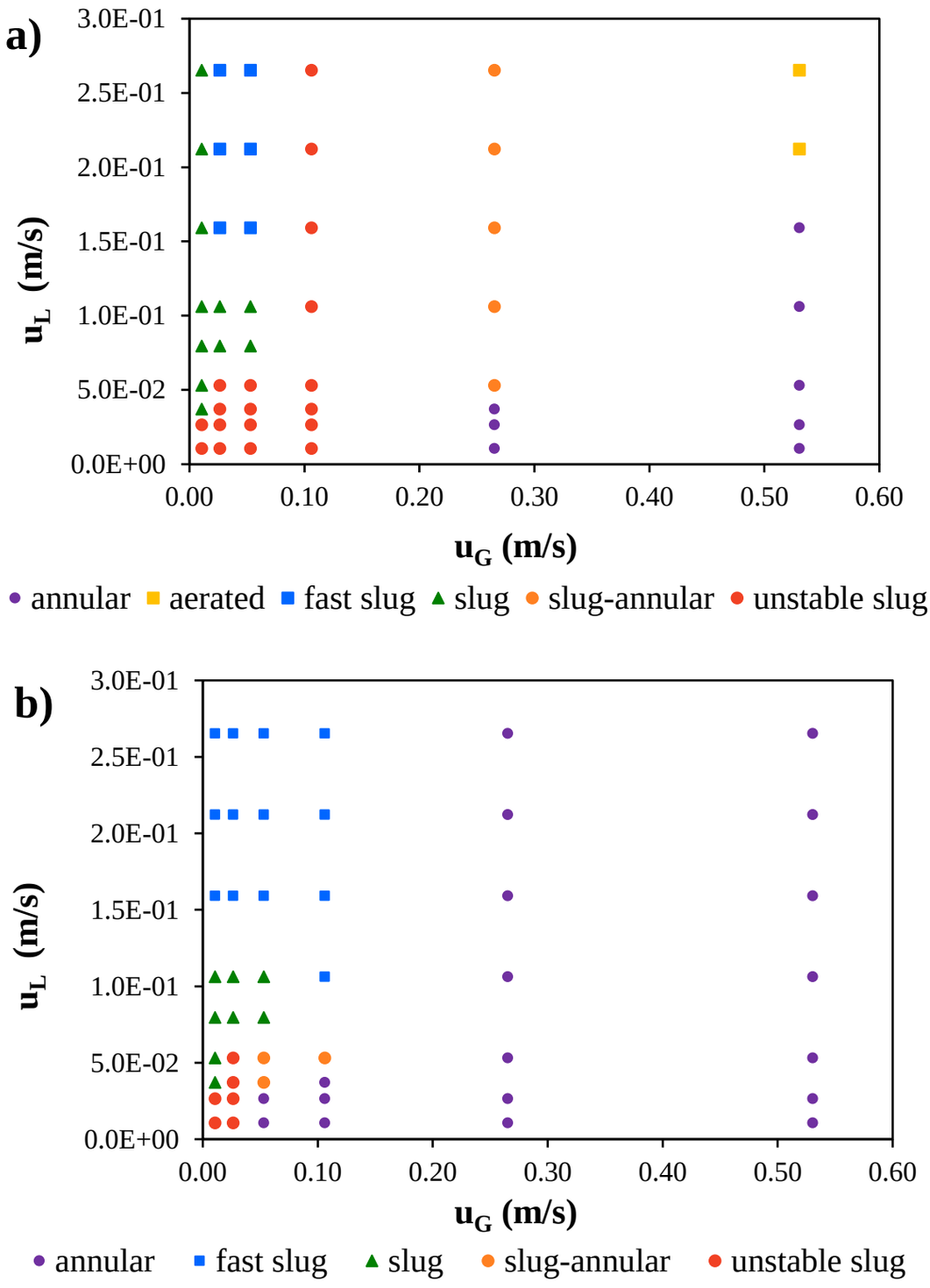

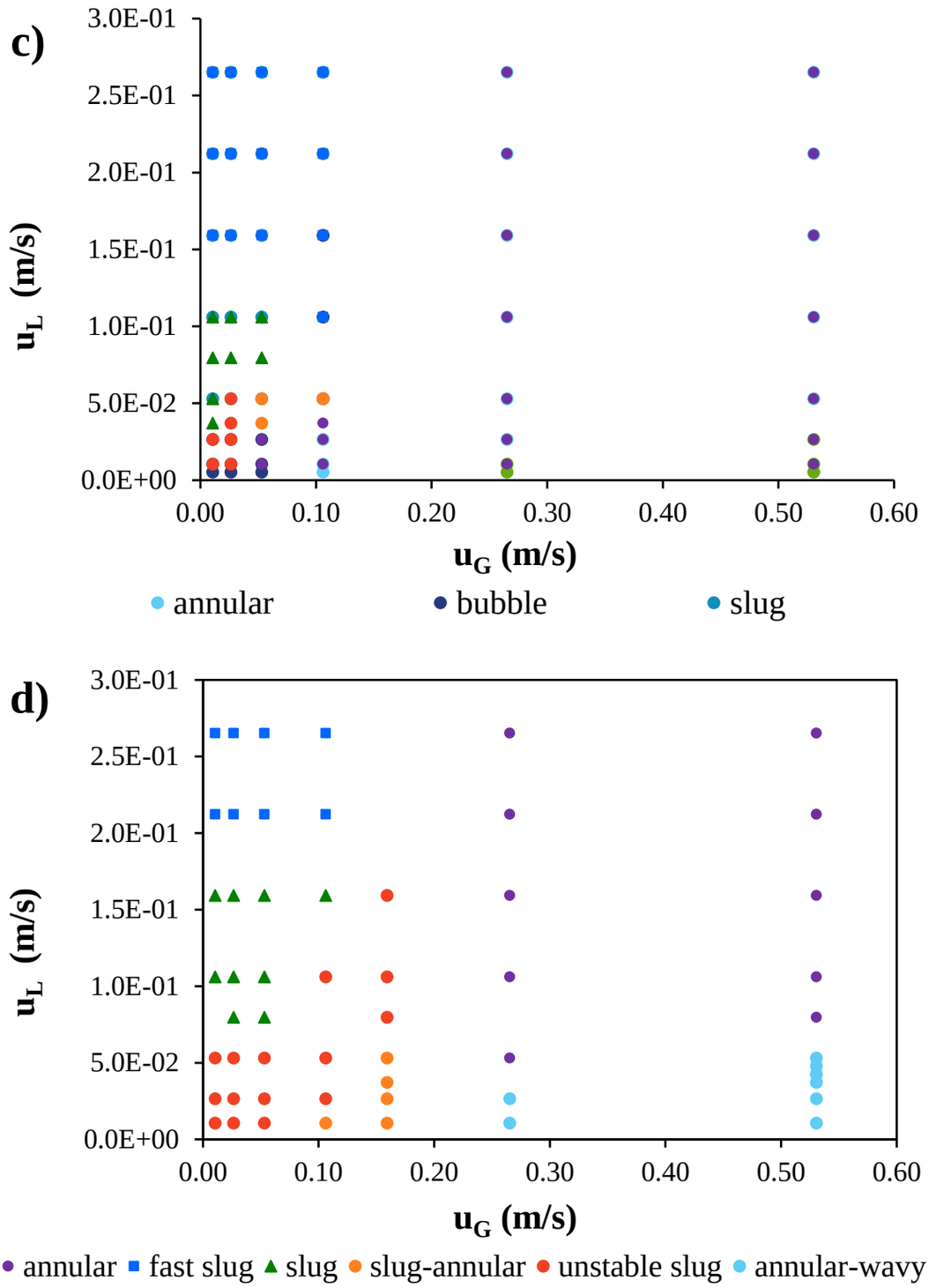

Source: "Elaborated by the author"

Table 4.1 Gas and liquid surface velocity operating window in the 300 mm length, 3 mm internal diameter capillary

Temperature, °C	Liquid phase	Operation window, m/s
10/ 25	Water	$1x10^{-2}<u_G<5x10^{-2}$, $7.9x10^{-2}<u_L<1.1x10^{-1}$
10	NaOH 0.5M	$1x10^{-2}<u_G<1x10^{-1}$, $5.3x10^{-2}<u_L<2.6x10^{-1}$
25	NaOH 0.5M	$1x10^{-2}<u_G<1x10^{-1}$, $7.9x10^{-2}<u_L<1.6x10^{-1}$

Source: "Elaborated by the author"

The established operational windows are very similar to those reported by Hurtado Alva, 2016; Hurtado, Solís-Casados, Escobar-Alarcón, Romero, & Natividad, 2016. In these studies the same type of capillaries was used and the established operating window was $1x10^{-2}<u_G<7x10^{-2}$ y $4x10^{-2}<u_L<5x10^{-1}$ m/s.

3.1.1 Effect of temperature on the hydrodinamics in the capillary reactor

According to Graphic 4.1, the temperature has a significant influence on the development of the type of regime in the capillaries. Using a temperature of 10 °C, there is a wider operating window to obtain the Taylor-type flow in both fluids (Graphic 4.1a and 4.1c) than operating at 25 °C (Graphic 4.1b and 4.1d) (values reported in Table 4.1) This is due to the fact that the formation of the Taylor-type regime is dominated by the forces of surface tension and viscosity, and therefore by temperature, since both physicochemical properties are dependent on it, as well as on the nature of the chemical solution. The lower the temperature, the higher the viscosity of the liquid and the greater the resistance of the liquid to flow in the capillary wall. The values of the different dimensionless numbers that affect the process are presented in Table 4.2.

Table 4.2 Reynolds, Schmidt and capillary numbers in the system CO_2-H_2O

Temperature, °C	Re_L	Re_G	Sc_L	Ca
10	182.4	21.3	1031.9	0.00139
25	267.1	19.5	455.9	0.00097
35	329.6	18.7	288.9	0.00081

Source: "Elaborated by the author"

The Reynolds numbers of liquid and gas indicate that both flows are under a laminar regime, that is, in a direction perpendicular to the gas-liquid interface, which confirms the consideration that the species only move in one direction, when applying the equation of continuity in the cap and the film. Finally, the capillary number validates that the surface tension forces have a greater contribution to the Taylor-type flow pattern than the viscous forces, which indicates that as the capillary number increases, the liquid film formed between the capillary wall and the bubble increases in thickness.

3.2 CO_2 absorption in the capillary reactor

3.2.1 Effect of the temperature on the CO_2 chemical absorption

According to the absorption profile shown in Graphic 4.2, in the absorption process with reaction, the modification of the operation temperature does not present any effect, since, for the five temperatures, the absorption behavior of CO_2 in 0.5M NaOH is similar in terms of saturation concentration and time to reach equilibrium. The equilibrium concentration was approximately 470 mol/m^3 and the time to reach equilibrium was approximately 2 hours.

The explanation for this phenomenon lies in the fact that temperature affects both the rate of diffusion of gases in a liquid and the rate constant of reaction but in opposite ways. As the temperature increases, the collision of the gas molecules increases, decreasing their diffusion speed in the liquid phase and also increases the number of molecules with an energy equal to or greater than the activation energy, thereby increasing the number of effective collisions, increasing the reaction rate constant. For this reason, there is a compensation between reaction kinetics and mass transfer, and therefore there is no difference in chemical absorption profiles when changing temperature.

At the same time, it should be noted that the quantity of CO_2 at equilibrium increased indisputably in the process with chemical reaction (NaOH as reducing agent) with respect to the physical absorption process, in a ratio of 40:1 compared to the maximum absorption achieved at 10 °C in the physical process. Definitely, the use of 0.5M NaOH in chemical absorption shows better results than the use of water in physical absorption.

Graphic 4.2 Comparison of the CO_2 absorption profile in a) water and b) in 0.5M NaOH, using a quartz capillary (300 mm length and 3 mm internal diameter)

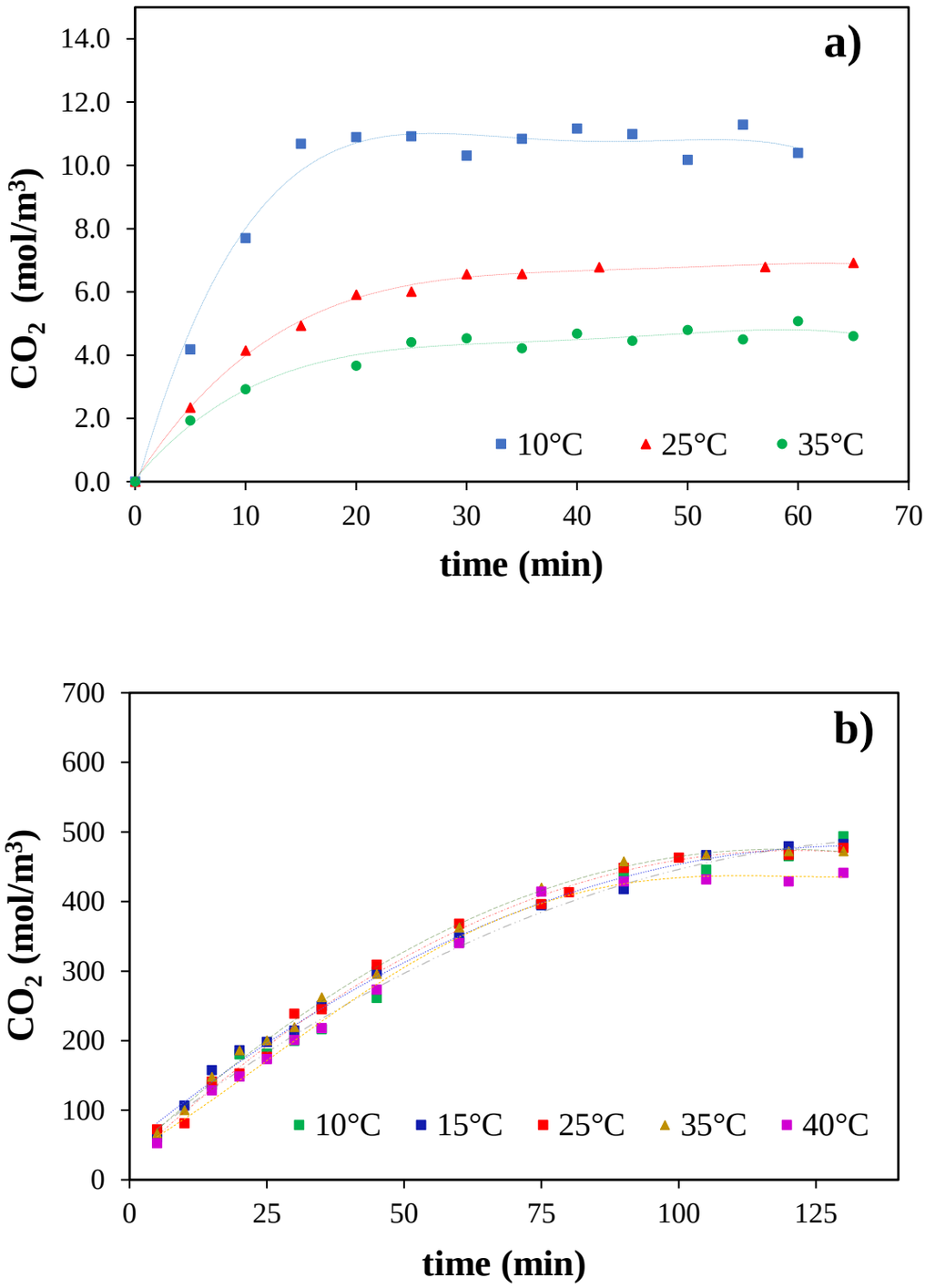

Source: "Elaborated by the author"

The pH of the liquid phase was measured during the absorption process. The profile obtained is shown in Graphic 4.3.

Graphic 4.3 Evolution of pH during CO_2 absorption in 0.5 M NaOH using a 3 x 300mm quartz capillary

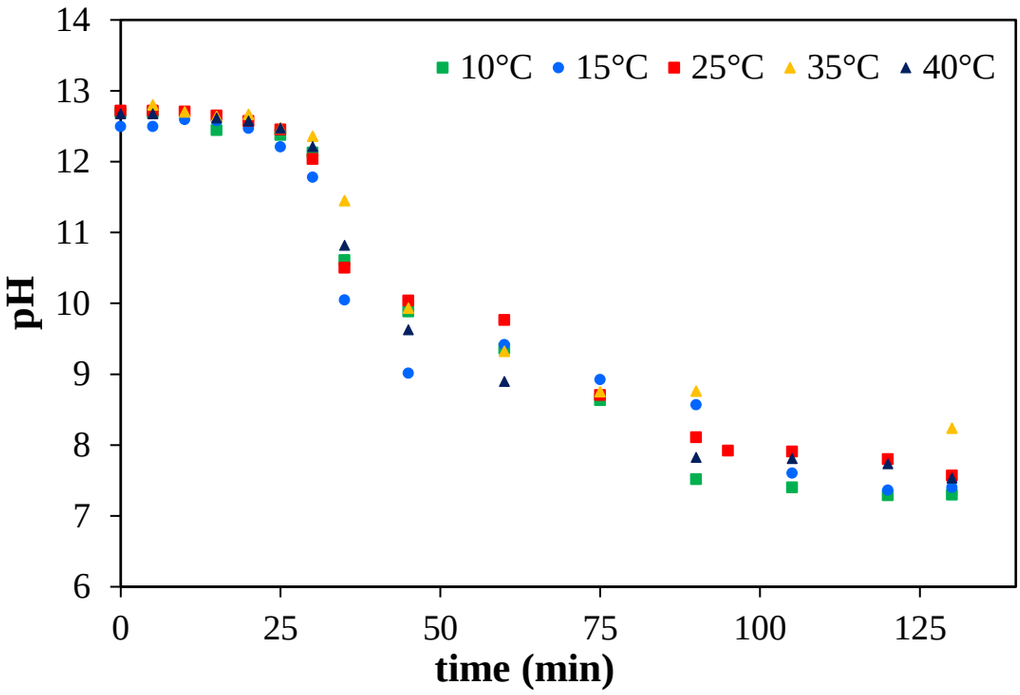

Source: "Elaborated by the author"

In Graphic 4.3, it can be observed that the pH follows the same trend in all cases. During the first two hours the pH decreases until it stabilizes at a pH around 7.5, regardless of the temperature tested. From the species distribution diagrams found in the literature (Ganesh, 2016), it can be inferred that the main chemical specie at the steady state is the bicarbonate ion. It can also be observed that at minute 35 a sudden drop in pH begins and it starts to stabilize at minute 65. After one hour and a half, a greater stability is observed in the curve, which is an indicative of the equilibrium condition.

This behavior coincides with the absorption profiles shown in Graphic 4.2b, so carrying out the pH monitoring to establish the time in which the steady state is achieved in the process is essential in addition to establish the concentration of species that participate in the reaction.

On the other hand, the abrupt drop in pH is a suggestion that the concentration of OH^- ions is rapidly reduced. Since the OH^- ions initially available in the medium are in excess, the reaction with CO_2 is fast during the first minutes causing the reduction of the OH^- ions and the formation of the carbonate ions (CO_3^{2-}). Once the available OH^- are consumed, the formation of bicarbonate ions begins at around a pH of 10.0. This trend is in concordance with the species distribution diagram reported by Ganesh, 2016.

3.2.2 Effect of NaOH concentration on the CO_2 absorption

Since the chemical absorption of CO_2 is influenced by the presence of the amount of OH^- ions available, experiments were carried out modifying the concentration of NaOH. Three concentrations were tested: 0.25M, 0.5M and 0.75M and the results obtained are shown in Graphic 4.4.

Graphic 4.4 CO_2 absorption profile in NaOH 0.25M, 0.5M and 0.75M

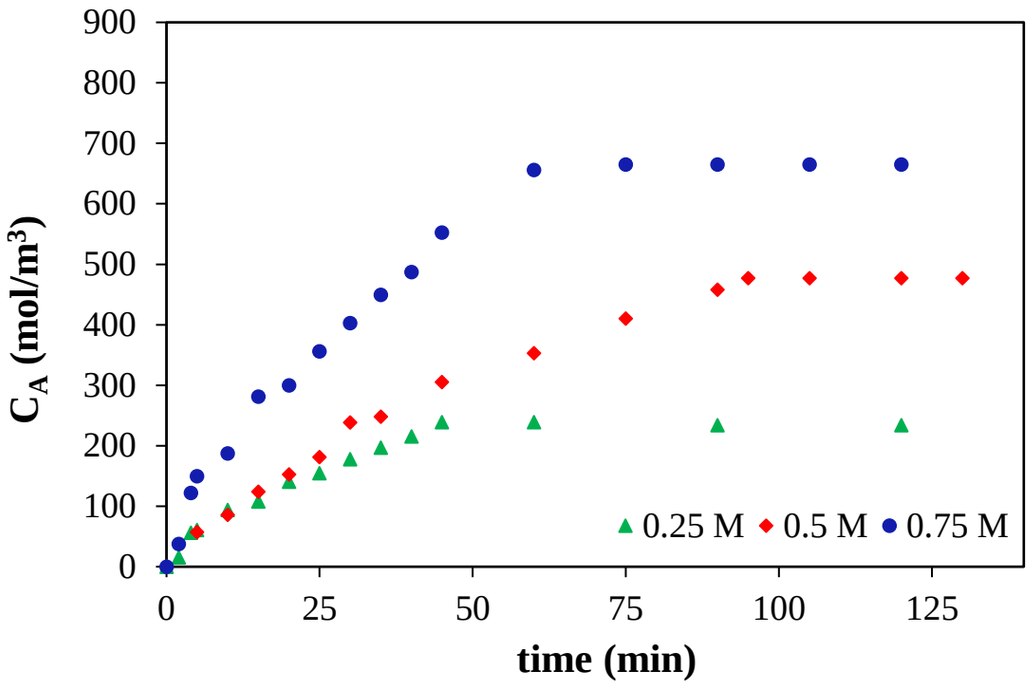

Source: "Elaborated by the author"

The greater availability of OH^- ions with a NaOH concentration of 0.75M, contributes to extend the stage where the chemical reaction of CO_2 with the OH^- ions takes place (initial slope of the curve) and a concentration of saturation greater than when using a NaOH concentration of 0.5M is also reached. A CO_2 concentration equal to 665 mol/m^3 was achieved, representing a greater amount of reactant available for its transformation to organic chemical species. It is also inferred that once the steady state is accomplished, in any of the cases, the only phenomenon is the mass transfer because there are not more OH^- ions to react with and this favors the formation of bicarbonate ions (via Equation 9) with the carbonate ions that were formed in Equation 8.

The pH profile of the solution during two hours of the experiment with different concentrations of NaOH is shown in Graphic 4.5. There is variation in the pH measured at the end of the experiment and this is related to the species that have been formed in the chemical absorption at the steady state. As indicated in section 3.4, the bicarbonate formed either by the dissociation of carbonic acid or by reaction with the hydroxyl ion (Equation 3 and Equation 6) is quickly consumed once it is formed, to generate carbonates until the ions OH^- are completely consumed (Equation 7); then bicarbonates are produced (Equation 9) until reaching the steady state.

Therefore, a final pH of 8.7, 7.6 and 7.0 was obtained in the solutions from higher to lower concentration of NaOH, respectively, and this value keeps a direct relationship with the bicarbonate ions concentration at the end of the process.

Graphic 4.5 Effect of NaOH concentration on the pH temporary profile during CO_2 absorption

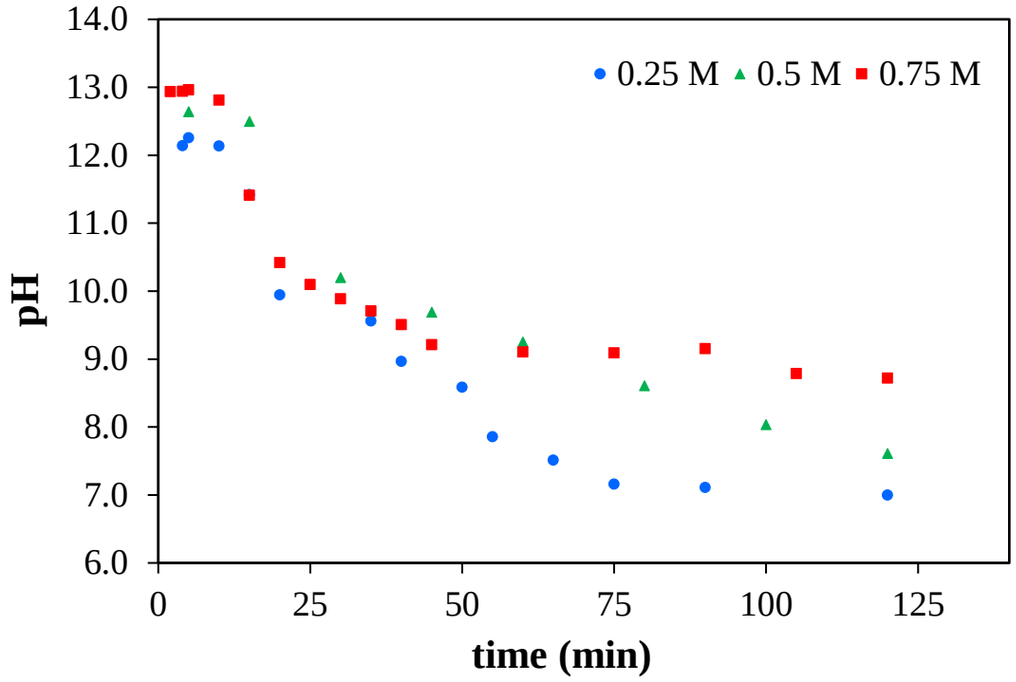

Source: "Elaborated by the author"

3.2.3 Effect of the length of the capillary reactor on the absorption of CO_2

Another important factor to study was the length of the capillary reactor (quartz capillary), assuming that modifying the residence time of the reactants within the capillary would have an effect on the absorbed amount of CO_2. An experiment was carried out using a 100 mm capillary instead of 300 mm, keeping the internal diameter of 3mm, the results are shown in Graphic 4.6.

Graphic 4.6 Effect of the capillary length on CO_2 absorption in NaOH 0.5 M at 25°C

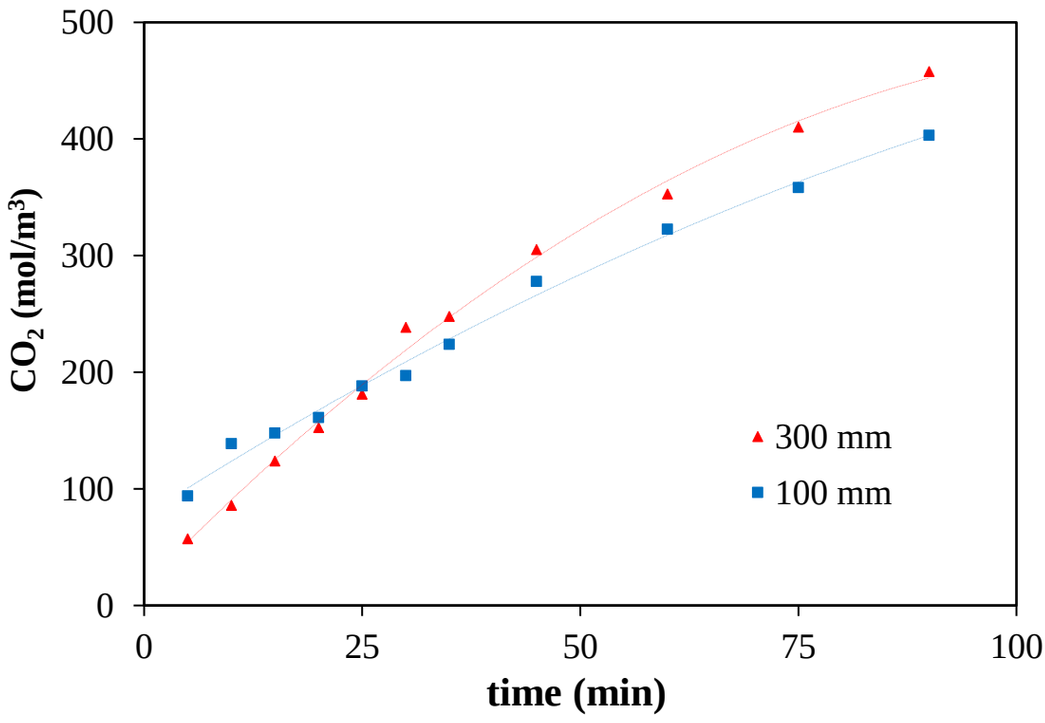

Source: "Elaborated by the author"

The concentration of saturation in the capillary of 100 mm reached 403 mol/m^3, in 90 minutes, which implies a decrease of 14% for the concentration obtained with the capillary of 300 mm, in the same period. This difference is considered as significant since the determined error is 0.47%. This result suggests that the residence time of the reactants is an important variable influencing the amount of CO_2 absorbed.

3.3 Determination of mass transfer coefficients

Physical absorption

For the determination of the mass transfer coefficient in the absorption with water, some considerations were made. Performing the molar flow balance in the system, we arrive at the continuity equation for a component in a binary mixture (Equation 10), which describes the variation of the concentration of a component with respect to time for a given point in space (Fogler, 2008),

$$D_{AB}\left[\frac{\partial^2 C_A}{\partial x^2}+\frac{\partial^2 C_A}{\partial y^2}+\frac{\partial^2 C_A}{\partial z^2}\right]-U_x\frac{\partial C_A}{\partial x}-U_y\frac{\partial C_A}{\partial y}-U_z\frac{\partial C_A}{\partial z}+r_A=\frac{\partial C_A}{\partial t} \quad (10)$$

This equation has been simplified, according to film theory, by assuming that the mass transfer occurs only in one direction by diffusion, in a gas-liquid system with two films, one for each phase, and stationary state; that is, the concentration of CO_2 in the liquid phase does not vary during the contact time between the gas phase of the bubble and the liquid phase, since the CO_2 is absorbed relatively slowly in water. The volumetric movement is too small to influence the diffusion of gases has also been considered (Beltrán, 2003). The equation has been reduced to a single term (Equation 11), with the boundary conditions indicated below,

$$D_{AB}\frac{d^2C_A}{dx^2}=0 \quad (11)$$

$$x=0;\ C_A=C_A^*$$
$$x=\delta;\ C_A=C_{Ab}$$

and it was related to Fick's first law, obtaining the following equation:

$$A_s N_i=\frac{d}{dt}V_c C_A=A_s k_L^0(C_e-C_{Ab}) \quad (12)$$

$$k_L^0=\frac{D_{AB}}{\delta} \quad (13)$$

Where:
A_s = Contact area between phases
N_i = Molar flux
V_c = Microreactor volume (capillary)
C_A = CO_2 concentration (variable)
k_L^0 = Mass transfer coefficient for physical absorption (in water)
C_e = Equilibrium concentration in liquid phase
C_{Ab} = CO_2 concentration at equilibrium (saturation)
D_{AB} = Diffusion coefficient of CO_2 – water system
δ = film thickness

Since the volume of the capillary reactor, V_c, is considered constant, the Equation 14 is obtained,

$$\frac{dC_A}{dt}=k_L^0 a(C_e-C_{Ab}) \quad (14)$$

Chemical absorption

In the Taylor-type regime, the mass transfer from the bubble to the gas-liquid interface can be neglected if the gas phase is pure CO_2, so the contribution is due only to the processes that occur within the liquid phase.

Furthermore, it is considered that the speed with which CO_2 diffuses into the liquid is the same which OH^- ions diffuse to the area where they are consumed. Applying the continuity equation to both CO_2 (species A) and OH^- ions (species B) and considering that they move in the x direction, the chemical absorption of CO_2 is described with Equations 15 and 16 (Nijsing, 1959; Beltrán, 2004)

$$\frac{\partial C_A}{\partial t} = \mathcal{D}_A \frac{\partial^2 C_A}{dx^2} - k_B C_B C_A \tag{15}$$

$$\frac{\partial C_B}{\partial t} = \mathcal{D}_B \frac{\partial^2 C_B}{dx^2} - k_B C_B C_A \tag{16}$$

This system of differential equations has an infinite number of solutions, the initial and boundary conditions were established,

$$t = 0,\ x \geq 0,\ C_A = 0\ ,\quad C_B = C_{B,0}$$

$$x = 0,\ t > 0,\ C_A = C_A^i\ ,\quad \frac{\partial C_B}{\partial x} = 0$$

$$x = \infty,\ t \geq 0,\quad C_A = 0,\quad C_B = C_{B,0}$$

A general solution makes use of the term improvement factor (Φ), which is based on the relationship between the mass transfer coefficient for chemical absorption (k_L) and that of physical absorption (k_L^0) (Perry, Green, & Maloney, 1992). The solution is a function of the Hatta number (Ha), the relationship between the initial OH^- concentration and the CO_2 concentration at the interface, and the relationship between the diffusivities of OH^- and CO_2 ions in water. Hatta is a dimensionless number that relates the rate of reaction in a liquid film to the rate of diffusion through the film (Beltrán, 2003) and is calculated as follows,

$$Ha = \frac{\sqrt{k_B C_{B,0} \mathcal{D}_{AB}}}{k_L^0} \tag{17}$$

On the other hand, it is necessary to know the reaction rate constant to determine the mass transfer coefficient. Regarding the order of reaction, two cases have been proposed, among several:

a. Pseudo-first order reaction, when C_B is too large compared to C^i_A and its diffusion rate to the reaction zone is very fast compared to the rate at which it is consumed in the reaction.
b. Second order reaction (extremely fast), when C_B is not so large compared to C^i_A and both species diffuse towards areas where their concentrations are lower.

With regard to reaction kinetics, it has been widely reported that the kinetic constant depends on the reaction temperature, the ionic strength of the solution, and the nature of the cation (Danckwerts & Kennedy, 1958; Harish Ganapathy, Al-hajri, & Ohadi, 2013; Grzelka *et al*., 2011; Pohorecki & Moniuk, 1988). Therefore, the equation proposed by Pohorecki & Moniuk, 1988 (Equation 18) was used to estimate the value of the kinetic constant in the chemical absorption of CO_2 in aqueous electrolyte solutions, in this equation, the kinetic constant depends on the temperature (T) and the ionic strength (I),

$$log_{10}(k_B) = 11.916 - \frac{2382}{T} + 0.221I - 0.016I^2 \tag{18}$$

The ionic strength is calculated with the molar concentration of the ions (C_i) present and their respective valence (z_i), characteristic of each ion, as indicates Equation 19.

$$I = 0.5 \sum_i C_i z_i^2 \tag{19}$$

In this study, during physical absorption (k_L^0), Equation 14 was used to estimate the mass transfer coefficient, using the slope of the straight line of the absorption profiles when using water as absorbent (data from Graphic 4.2a). Graphic 4.7 shows the trend lines for each temperature and Table 4.3 shows the results of the volumetric mass transfer coefficient for each temperature as well as the coefficients of determination (R^2) for each trend line.

It is worth commenting that when carrying out the experiments, the concentration of initial CO_2 in the liquid solution (blank) was disregarded from each value, so the initial conditions are $t = 0,\ C_A = 0$, the coefficient of determination in Table 4.3 tells the data fit well to the lineal model and is higher when temperature increases (with $p<0.05$) for the three temperatures.

Graphic 4.7 Graph for the calculation of the volumetric mass transfer coefficient in the CO_2-H_2O system

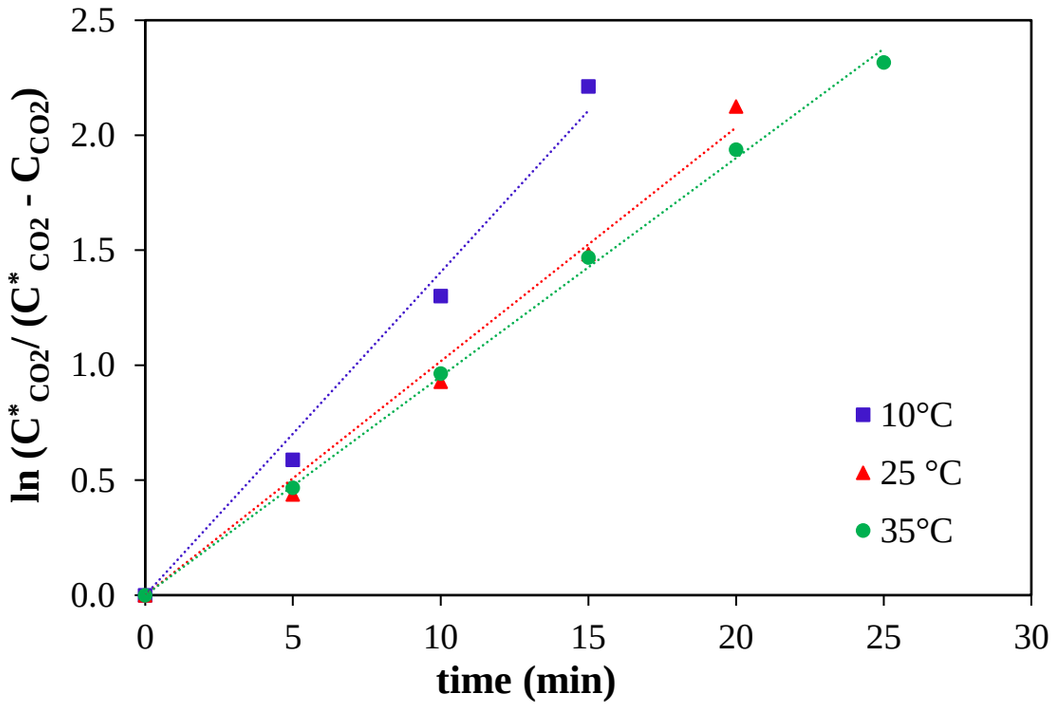

Source: "Elaborated by the author"

Table 4.3 Determination coefficient and slope of the linear equations plotted in Graphic 7

Temperature, °C	Time to reach equilibrium, minutes	Slope = k_L^0a, s^{-1}	Determination coefficient, R^2	p-value
10	15	0.00234	0.987	<0.005
25	20	0.00169	0.992	<0.0002
35	25	0.00158	0.998	<0.0002

Source: "Elaborated by the author"

In Table 4.3, it can be seen that the value of the volumetric mass transfer coefficient (k_L^0a) increases when the temperature decreases, and this behavior is in concordance with the fact that the solubility of CO_2 increases when the temperature decreases (Henry's Law). Empirical correlations reported in the literature were used to compare the volumetric mass transfer coefficients with those determined in this study during the absorption of CO_2 in water. Table 4.4 presents a comparison of the results. It can be seen that the experimental data obtained fit very well with the correlation of H. Ganapathy, Shooshtari, Dessiatoun, Ohadi, & Alshehhi, 2015. It is important to specify that in all the cases, in the literature reported in Table 4, the flow channels had a smaller diameter than that used in this study by at least one order of magnitude, also the length.

Table 4.4 Determination of mass transfer coefficients using correlations reported in the literature

Temperature, °C	k_La, experimental	Yue, 2007	Kuhn and Jensen, 2012	Yao, 2015	Ganapathy, 2015
10	0.00234	0.14378	0.000145	0.044193	0.00227
25	0.00169	0.20725	0.000128	0.019798	0.00111
35	0.00158	0.25464	0.000123	0.012934	0.00075

Source: "Elaborated by the author"

The results of the reaction rate constant and the mass transfer coefficient when performing chemical absorption are shown in Table 4.5. The Hatta number relates the rate of reaction in a liquid film to the rate of diffusion through the film and indicates whether or not the reaction occurs faster than the mass transfer, identifying the controlling step of the absorption process.

Table 4.5 Kinetic and mass transfer coefficients obtained in the chemical absorption process of CO_2 in 0.5M NaOH

Temperature	10°C	25°C	35°C
Ha	47.0	72.7	127.1
k_B (m^3/mol s)	0.0372	0.0551	0.0716
k_L x 10^5 (m/s)	3.381	2.831	2.296
k^0_L x 10^6 (m/s)	1.657	1.272	9.939
k_L/k^0_L	20	22	23

Source: "Elaborated by the author"

The Ha values shown in Table 4.5, indicate that the chemical reaction is much faster than diffusion, and therefore, the absorption process is controlled by mass transfer. The behavior observed in the CO_2 absorption profiles obtained by modifying the NaOH concentration in the solution (Graphic 4.4) is consistent with the previous statement: on the initial slope of the absorption profile curve, the OH^- ions are found in excess and all absorbed CO_2 reacts immediately, in contrast, later the concentration of OH^- ions decreases and this chemical species is no longer available to react with the CO_2 molecules at the interface.

As for the kinetic constant, k_B, it is observed that it increases proportionally with temperature, since the increase in temperature affects the activation energy of the molecules. The value of the mass transfer coefficient, k_L, decreases with increasing temperature and this behavior is consistent with that reported in the literature. These results confirm that there is a compensation between the chemical reaction and the mass transfer in the process of chemical absorption of CO_2 in the 0.5 M NaOH solution when carried out at different temperatures. As the temperature increases, the OH^- ions and CO_2 in the reaction are activated more quickly, however, the increase in temperature represents a lower availability of OH^- ions due to the low solubility and molecular diffusion.

In this way, there is a compensation in both phenomena (while one grows the other decreases due to the effect of temperature) obtaining similar absorption profiles (Graphic 4.2). Another important point to conclude besides that the use of a NaOH solution improves the absorption process of CO_2 in water, is the relationship between the mass transfer coefficient with chemical absorption and that of physical absorption, which is approximately 20 times higher.

From the results of Table 4.6, when modifying the concentration of NaOH in the solution, no significant effect is observed in the reaction rate constant (k_B), since the kinetic constants for the three concentrations are similar. This indicates that the rate at which the OH^- ions is consumed is similar, regardless of whether there is a greater quantity of them as their concentration increases. However, there is a very slight increase in the mass transfer constant (k_L) when the concentration of the ions increases, which indicates that having more ions leads to a better mass transfer.

Table 4.6 Kinetic and mass transfer coefficients obtained at 25 ° C in the process of chemical absorption of CO_2 in NaOH solutions with concentrations of 0.25, 0.5 and 0.75M

NaOH concentration	0.25M	0.5M	0.75M
Ha	40.5	72.7	103.1
k_B (m^3/mol s)	0.0537	0.0551	0.0573
k_L x 10^5 (m/s)	2.466	2.83	2.924
k^0_L x 10^6 (m/s)	1.272	1.272	1.272
k_L/k^0_L	19	22	23

Source: "Elaborated by the author"

3.4 Variation of involved species

During the absorption process with chemical reaction, in addition to the CO_2 dissolved in the liquid phase, other ions are also present, such as bicarbonate and carbonate (HCO_3^- and CO_3^{2-}). Graphic 4.8 shows the evolution of the concentration of the species involved in the process over time for NaOH concentrations 0.25, 0.5 and 0.75M at 25 °C as well as the evolution of pH. In Graphic 4.8, we can see that, when consuming NaOH, due to the reaction with CO_2, carbonate ions begin to be generated until reaching a maximum concentration. The experimental relationship between the concentration of hydroxide and carbonate is 2:1 as shown in Graphic 4.8 a, c and d, which coincides with the stoichiometry of the reaction (Equation 8), obtaining molar yields of almost 100%. Once the hydroxyl ion has been used up, the formed carbonate begins to react with CO_2 to produce the bicarbonate ion, which is the final product of the general reaction (Equation 9). Once the carbonate is depleted in reactive absorption to produce bicarbonate, then the physical absorption of CO_2 begins. This, considering that the absorption of CO_2 implies, on the one hand, the reaction rate and, on the other, the diffusion of the OH^- ions; consequently, only the mass transfer prevails once the concentration of OH^- ions is minimum.

In Graphic 4.8b, d and e, it is identified that the predominance of the reaction to form bicarbonate (Equation 6) occurs when the pH is greater than 10 in the hydroxide/carbonate mixture, due to the instantaneous reaction to form carbonate (Equation 7). The carbonate is formed instantly once a bicarbonate ion is generated; thus, the generation of bicarbonate is appreciated until the production of carbonate ends due to the depletion of the OH^- ions, most of the carbonate/bicarbonate mixtures occur between a pH from 8-10.5. Likewise, it can be observed that the pH tends to stabilize when all the carbonate has reacted and has become bicarbonate (pH approximately 8). This indicates that the final solution is a saturated solution where is no longer possible to continue chemically absorbing CO_2 given the carbonic acid/bicarbonate balance in physical absorption (Equation 3). Recapitulating, the bicarbonate ion generated by the dissociation of carbonic acid and also by the presence of the hydroxyl ion (Equation 3 and Equation 6) is consumed immediately once it is formed, as they are quite fast reactions, for the generation of carbonate until all are exhausted. The OH^- ions (Equation 7), from that moment on, bicarbonates will be produced (Equation 6), until equilibrium is reached. The time in which the OH^- is depleted depends on its concentration: the higher the concentration, the longer the period of time during which the reaction between CO_2 and OH^- occurs. Finally, it only remains to point out the importance of constant monitoring of pH in this type of process, since from the slopes in its temporal profile, the beginning and end of each of the reactions in which CO_2 participates in solutions can be inferred until it reaches equilibrium.

Graphic 4.8 Chemical Species Concentration and pH temporary profiles in the CO_2 absorption process at 25 °C

a) C*i* in NaOH 0.25M

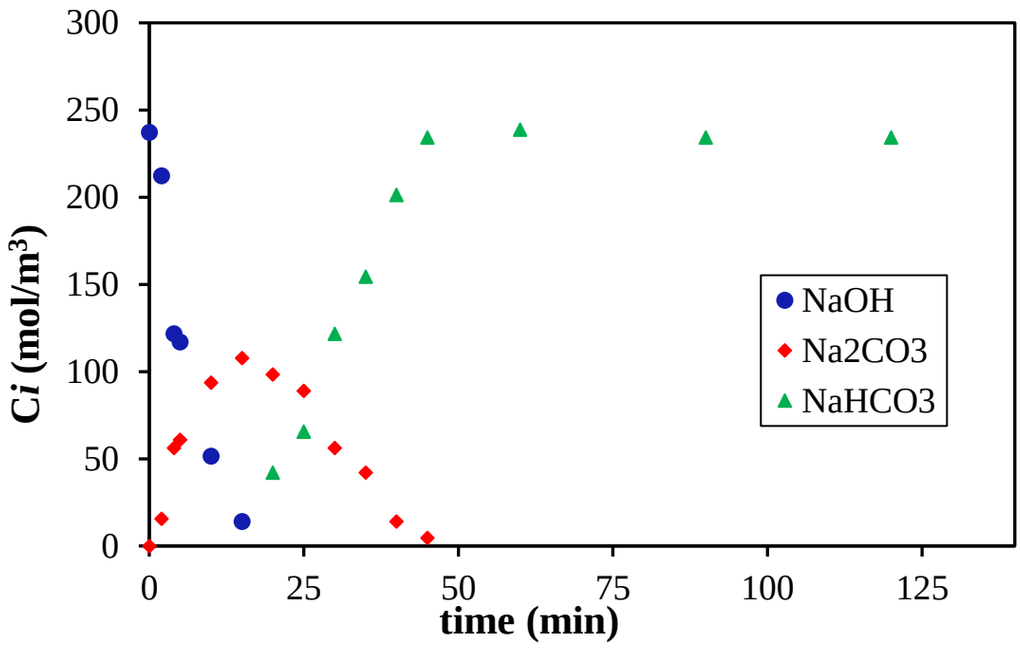

b) pH in NaOH 0.25M

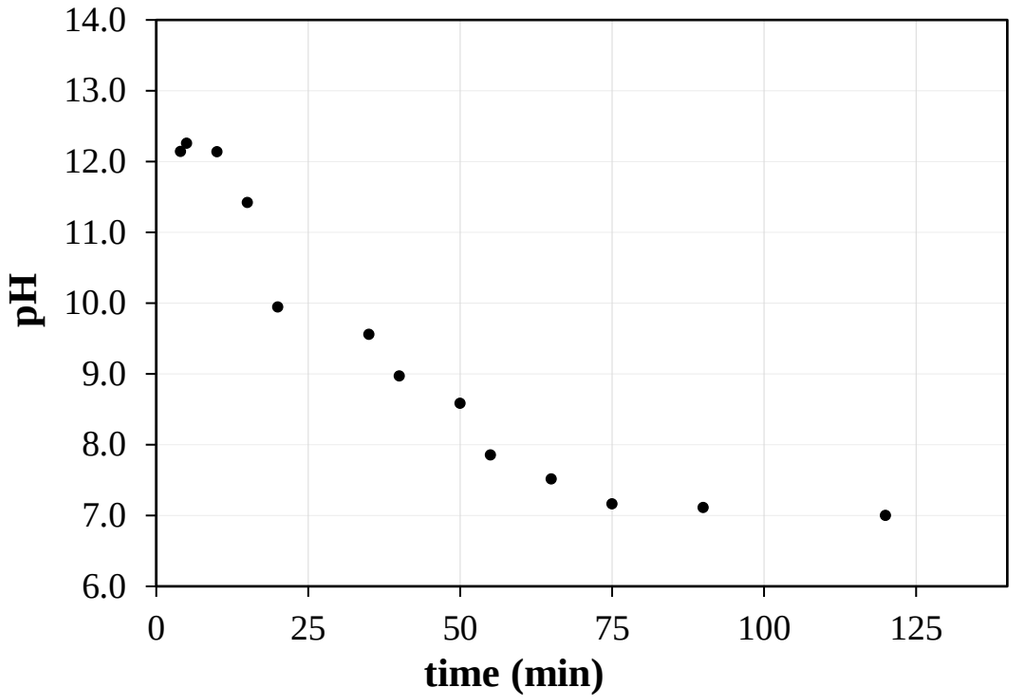

c) C*i* in NaOH 0.5M

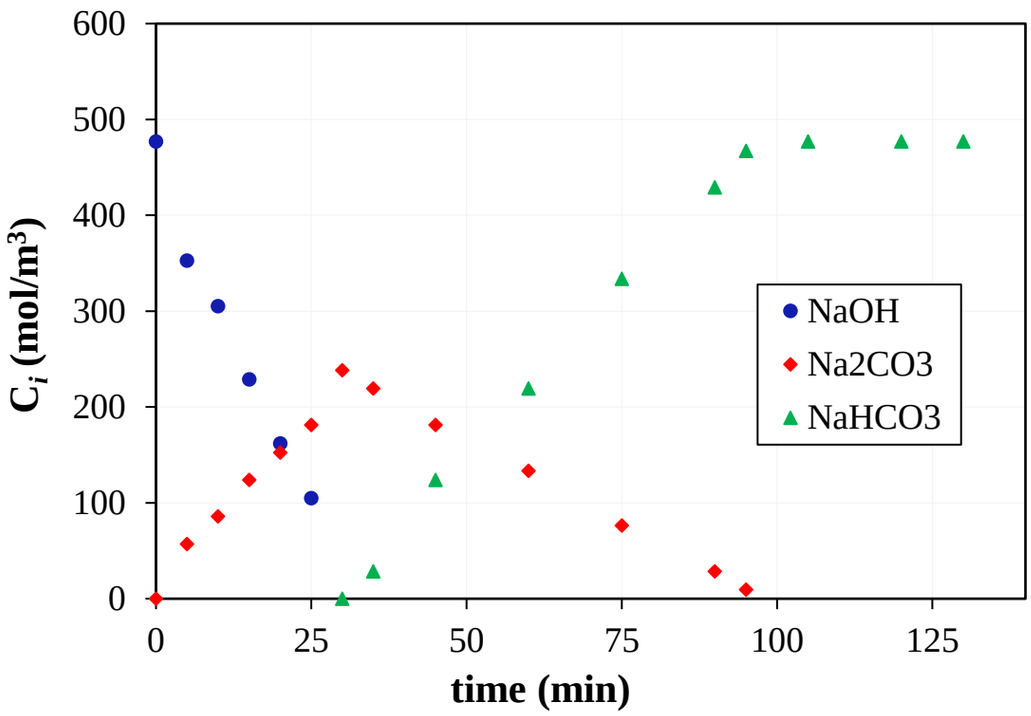

d) pH in NaOH 0.5M

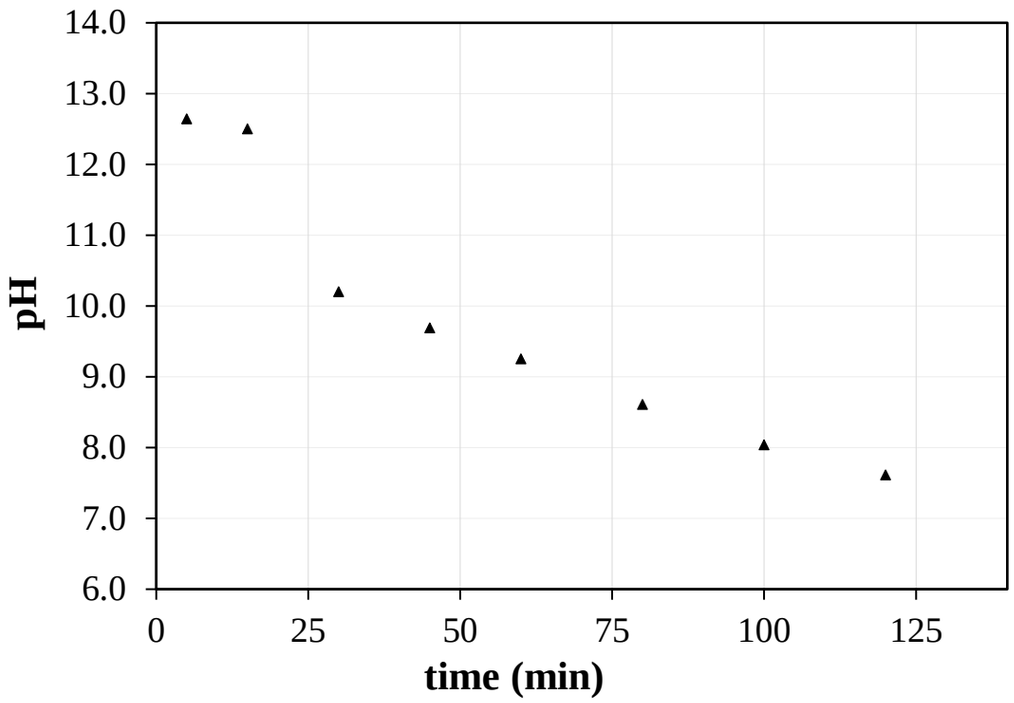

e) C*i* in NaOH 0.75M

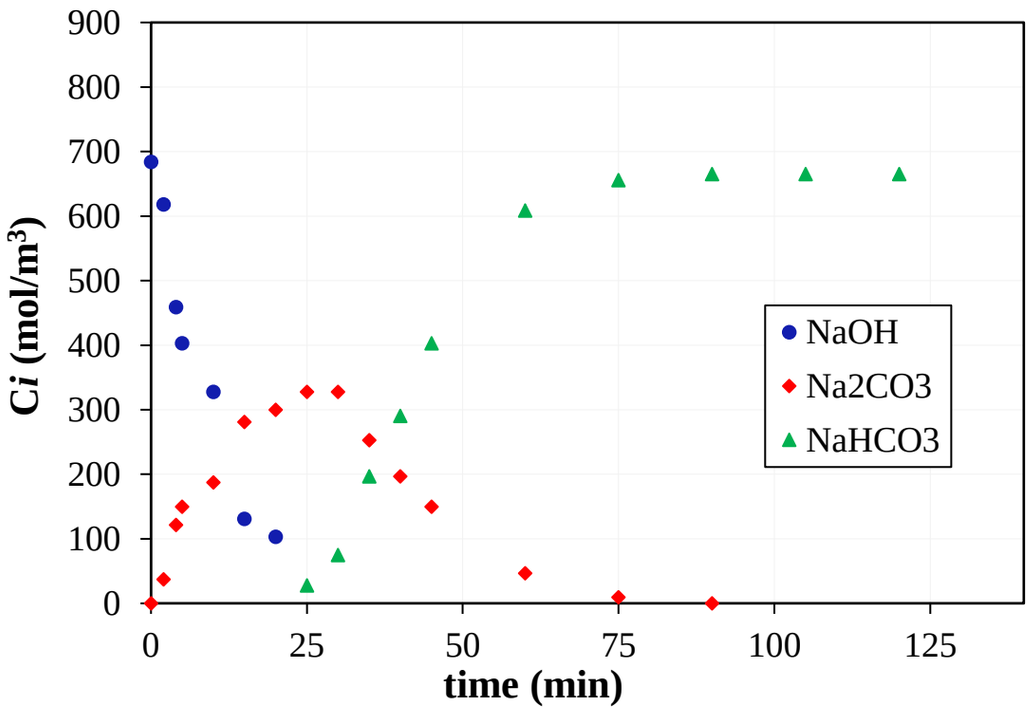

f) pH in NaOH 0.75M

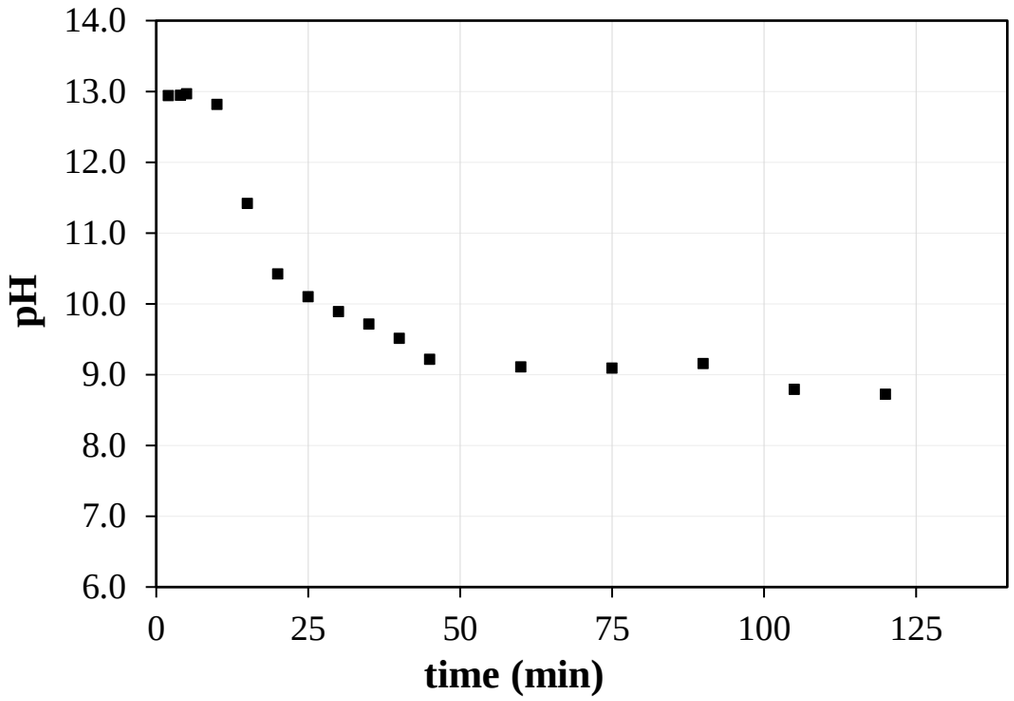

Source: "Elaborated by the author"

4. Acknowledgments

Rosaura Peña thanks the National Council of Science and Technology (CONACyT) for the financial support through scholarship No. 239954 to conduct doctoral studies. Authors also thank CONACyT for the project No. 269093 and Universidad Autónoma del Estado de México for project 6235/2020CIB. Authors also would like to thank Citlalit Martínez Soto for technical support.

5. Conclusions

- The operating window of the gas and liquid surface velocity to obtain the Taylor-type regime, at 10 ° C in a capillary with 3mm internal diameter is $1x10^{-2} < u_G < 5x10^{-2}$ and $7.9x10^{-2} < u_L < 1.1x10^{-1}$ m/s, using water and 0.5M NaOH, respectively.

- The operating window of the gas and liquid surface velocity to obtain the Taylor-type regime, at 25 ° C in a capillary with 3mm internal diameter is $1x10^{-2} < u_G < 5x10^{-2}$ and $8x10^{-2} < u_L < 1.6x\ 10^{-1}$ m/s, using water and 0.5M NaOH, respectively.

- There is a greater absorption of CO_2 using alkaline solutions than using only water.

- The value of the volumetric mass transfer coefficient in the absorption of CO_2 with water, increases with decreasing temperature

- The mass transfer coefficient in the absorption of CO_2 with NaOH in solution increases directly with temperature.

- The combined method of titration and pH measurement allows monitoring the behavior of the different ionic species that can be generated during the absorption of CO_2 in alkaline solutions.

6. References

Beltrán, F. J. (2003). *Ozone reaction kinetics for water and wastewater systems*. Lewis Publishers.

Centi, G., & Perathoner, S. (2009). Opportunities and prospects in the chemical recycling of carbon dioxide to fuels. *Catalysis Today*, *148*(3–4), 191–205. https://doi.org/10.1016/j.cattod.2009.07.075

Cotton, F. A. et al. (1999). *Advanced inorganic chemistry* (6a ed.). Wiley.

Danckwerts, P. V., & Kennedy, A. M. (1958). The kinetics of absorption of carbon dioxide into neutral and alkaline solutions. *Chemical Engineering Science*, *8*(3–4), 201–215. https://doi.org/10.1016/0009-2509(58)85027-7

Fogler, H. S. (2008). *Elementos de ingeniería de las reacciones químicas* (4a ed.). México: PEARSON EDUCACIÓN.

Ganapathy, H, Shooshtari, A., Dessiatoun, S., Ohadi, M. M., & Alshehhi, M. (2015). Hydrodynamics and mass transfer performance of a microreactor for enhanced gas separation processes. *Chemical Engineering Journal*, *266*, 258–270.

Ganapathy, Harish, Al-hajri, E., & Ohadi, M. (2013). Mass transfer characteristics of gas – liquid absorption during Taylor fl ow in mini / microchannel reactors. *Chemical Engineering Science*, *101*, 69–80. https://doi.org/10.1016/j.ces.2013.06.005

Ganesh, I. (2016). Electrochemical conversion of carbon dioxide into renewable fuel chemicals – The role of nanomaterials and the commercialization. *Renewable and Sustainable Energy Reviews*, *59*, 1269–1297. https://doi.org/10.1016/j.rser.2016.01.026

Grzelka, J., Sobieszuk, P., Pohorecki, R., & Cygan, P. (2011). Determination of the interfacial area and mass transfer coefficients in the Taylor gas – liquid flow in a microchannel, *66*, 6048–6056. https://doi.org/10.1016/j.ces.2011.08.029

Heiszwolf, J. J., Kreutzer, M. T., Eijnden, M. G. Van Den, Kapteijn, F., & Moulijn, J. A. (2001). Gas – liquid mass transfer of aqueous Taylor flow in monoliths, *69*, 51–55.

Holum, J. R. (1990). *Principios de fisicoquímica, química orgánica y química*. México: Limusa.

Hurtado Alva, L. (2016). *Reactores capilares para fotosíntesis artificial*. Universidad Autónoma del Estado de México.

Hurtado, L., Solís-Casados, D., Escobar-Alarcón, L., Romero, R., & Natividad, R. (2016). Multiphase photo-capillary reactors coated with TiO_2 films: Preparation, characterization and photocatalytic performance. *Chemical Engineering Journal*, *304*, 39–47. https://doi.org/10.1016/j.cej.2016.06.003

Hurtado, Lourdes, Natividad, R., & García, H. (2016). Photocatalytic activity of Cu_2O supported on multi layers graphene for CO_2 reduction by water under batch and continuous flow. *Catalysis Communications*, *84*, 30–35.

Mebrahtu, C., Krebs, F., Abate, S., Perathoner, S., Centi, G., & Palkovits, R. (2019). and Challenges, *178*, 85–103.

Natividad, R., Kulkarni, R., Nuithitikul, K., Raymahasay, S., Wood, J., & Winterbottom, J. M. (2004). Analysis of the performance of single capillary and multiple capillary (monolith) reactors for the multiphase Pd-catalyzed hydrogenation of 2-butyne-1,4-diol. *Chemical Engineering Science*, *59*(22–23), 5431–5438. https://doi.org/10.1016/j.ces.2004.09.011

Ola, O., & Maroto-Valer, M. M. (2015). Review of material design and reactor engineering on TiO_2 photocatalysis for CO_2 reduction. *Journal of Photochemistry and Photobiology C: Photochemistry Reviews*, *24*, 16–42. https://doi.org/10.1016/j.jphotochemrev.2015.06.001

Palmer, D. A., & Van Eldik, R. (1983). The chemistry of metal carbonato and carbon dioxide complexes. *American Chemical Society*, *83*, 651–731.

Perry, R. H., Green, D. W., & Maloney, J. O. (1992). *Manual del ingeniero químico* (6a ed.). McGraw-Hill.

Pohorecki, R., & Moniuk, W. (1988). Kinetics of reaction between carbon dioxide and ions in aqueous electrolyte solutions. *Chemical Engineering Science*, *43*(7), 1677–1684.

Savage, D. W., Astarita, G., & Joshi, S. (1980). Chemical absorption and desorption of carbon dioxide from hot carbonate solutions. *Chemical Enginering Science*, *35*, 1513–1522.

Shehzad, N., Tahir, M., Johari, K., & Murugesan, T. (2018). A critical review on TiO_2 based photocatalytic CO_2 reduction system : Strategies to improve efficiency, *26*(May), 98–122. https://doi.org/10.1016/j.jcou.2018.04.026

Shim, J.-G., Lee, D. W., Lee, J. H., & Kwak, N.-S. (2016). Experimental study on capture of carbon dioxide and production of sodium bicarbonate from sodium hydroxide. *Environmental Engineering Research*, *21*, 297–303.

Skoog, D. R. (2014). *Fundamentals of analytical chemistry* (9th ed.). CENGAGE Learning.

Yang, H., Zhang, C., Gao, P., Wang, H., Li, X., Zhong, L., Sun, Y. (2017). A review of the catalytic hydrogenation of carbon dioxide into value-added hydrocarbons. *Catalysis Science and Technology*, *7*(20), 4580–4598. https://doi.org/10.1039/c7cy01403a